Available online at www.sciencedirect.com

ScienceDirect

Ceramics International 40 (2014) 3981–3988

CERAMICS INTERNATIONAL

www.elsevier.com/locate/ceramint

Hydrothermal assisted synthesis and hot-corrosion resistance of nano lanthanum zirconate particles

Chaohui Wang[a,b], You Wang[a,*], Liang Wang[c], Xiaoguang Sun[a], Changlong Yang[b], Zhiwei Zou[a], Xuewei Li[a]

[a]*Laboratory of Nano Surface Engineering, School of Materials Science and Engineering, Harbin Institute of Technology, Harbin 150001 PR China*
[b]*College of Materials Science and Engineering, Qiqihar University, Qiqihar 161006 PR China*
[c]*Key Laboratory of Inorganic Coating Materials, Shanghai Institute of Ceramics, Chinese Academy of Sciences, Shanghai 201899 PR China*

Received 1 July 2013; received in revised form 9 August 2013; accepted 9 August 2013
Available online 16 August 2013

Abstract

The nano $La_2Zr_2O_7$ (LZ) particles with pyrochlore microstructure were successfully synthesized from a mixture of $La(NO_3)_3$, $Zr(NO_3)_4$ and $C_{19}H_{42}BrN$ (CTAB) using hydrothermal assisted (HTA) synthesis which consists of two steps: hydrothermal treatment and calcination. Transmission electron microscopy (TEM), scanning electron microscopy (SEM), Fourier transform infrared spectra (FT-IR) and X-ray diffraction (XRD) spectroscopy were employed to study morphologies and phase compositions. The results suggest that HTA process led to very rapid synthesis of nano LZ compared to the conventional solid reaction process. The particles produced by HTA synthesis have cubic shape and the distribution of its grain size is from 10 nm to 30 nm. The present work demonstrates that the nano $La_2Zr_2O_7$ produced via HTA synthesis which have better hot-corrosion resistance is an ideal material for thermal barrier coatings.

Keywords: Hydrothermal assisted synthesis; $La_2Zr_2O_7$; Nanoparticle; Hot corrosion

1. Introduction

In recent years, nanopyrochlore type oxide materials have received considerable attention due to its wide industrial application [1,2]. Pyrochlore type oxide (cubic, Fd3m) can be usually expressed by the general formula $A_2B_2O_7$ (A and B are trivalent and tetravalent metal ions). Pyrochlore type of rare earth zirconates ($Ln_2Zr_2O_7$, Ln denotes rare earth) has gained intense interest for their important technological applications. These zirconates exhibit low thermal conductivity, high melting point, thermal expansion coefficient [3,4], excellent photocatalytic activity [5], host materials for luminescence centers [6] and good dielectric property [7]. In view of such excellent properties, $Ln_2Zr_2O_7$ is widely used as thermal barrier coatings (TBCs), possible host for radioactive wastes and surplus actinides and solid electrolytes in high-temperature fuel cells [8]. In the series of the $Ln_2Zr_2O_7$, the $La_2Zr_2O_7$ (LZ) is the typical compound and has been widely used in the thermal barriers research and it has exhibited excellent thermal properties such as low thermal conductivity, high thermal stability and so on [9].

In order to obtain fine LZ crystalline particles which can be used for plasma spraying, various methods have been proposed. As we know, the LZ has been successfully prepared via the traditional high temperature solid-state reaction [10], but the heating temperature is almost above 1700 K and the average size of products may reach to a few microns. In order to obtain LZ coatings with better property, the nano LZ particles were widely synthesized by many methods such as co-precipitation [4], sol–gel [11], stearic acid combustion method [12], and salt-assisted combustion [13]. However, the particles prepared by the above methods were irregular in shape and inhomogeneous in size distribution. In the fabrication process of nanomaterials, the hydrothermal technique is

*Corresponding author at: Harbin Institute of Technology, School of Materials Science and Engineering, Laboratory of Nano Surface Engineering, No.92 West-Dazhi street, Harbin 150001, China. Tel.: +86 458 6402752; fax: +86 451 86402752.
E-mail addresses: wangchh8@gmail.com (C. Wang). wangyou@hit.edu.cn (Y. Wang).

0272-8842/$ - see front matter © 2013 Elsevier Ltd and Techna Group S.r.l. All rights reserved.
http://dx.doi.org/10.1016/j.ceramint.2013.08.048

promising, which can promote the reaction processing for the system activation has increased under the high temperature and high pressure subcritical conditions, and which is mentioned to have great potential for the near-room temperature manufacture of nanoparticles [14]. The main advantages of this method are related to the homogeneous nucleation processes and extra small grain size due to lower sinter temperature or the elimination of calcination step [15].

However, it is difficult to synthesis LZ only using the hydrothermal technique due to the slow reaction rate. After the hydrothermal treatment, a moderate heating at lower temperature could accelerate the solid reaction and control the particles size.

In the present works, nanocrystalline LZ particles were synthesized via the hydrothermal-assisted (HTA) method. The parameters in processing technique of LZ were be optimized, and properties of LZ particles were characterized in this paper. The study is also to evaluate the thermal corrosion properties of the as-prepared LZ produced by different methods.

2. Experimental procedure

2.1. Synthesis of nano LZ particles

The LZ particles with nanosize were prepared by the hydrothermal-assisted (HTA) method including two steps: hydrothermal treatment and high temperature solid reaction. The $La(NO_3)_3 \cdot 6H_2O$ (AR, Tianjin Kemiou Chemical Reagent Co., Ltd.) and $Zr(NO_3)_4 \cdot 5H_2O$ (AR, Tianjin Kemiou Chemical Reagent Co., Ltd.) were used as the precursors of the La^{3+} and Zr^{4+}, respectively. CTAB ($C_{19}H_{42}BrN$) (AR, Tianjin Kemiou Chemical Reagent Co., Ltd.) was used as a cationic surfactant. NaOH (AR, Tianjin Kemiou Chemical Reagent Co., Ltd.) solution was acted as a pH regulator.

The fabrication procedures are shown in Fig. 1. 10 ml 0.5 mol/L $La(NO_3)_3$ solution and 10 ml 0.5 mol/L $Zr(NO_3)_4$ solution were mixed in the vessel with the magnetic stirrer at room temperature, in which the 2 wt% surfactant CTAB was blended. The pH value of the mixture was regulated to 7 by dropwise adding the 0.1 mol/l NaOH solution. The mixture was added into the hydrothermal reactor, and the reactor was heated in the drying oven under certain temperature conditions for 24 h. Then it was cooled to the room temperature, the suspension mixture was taken out and centrifuged. The solid sediments were dried in the vacuum drying oven and ground to the fine particles in the agate mortar. Finally, the particles were calcined for 2 h in the electric furnace.

The particles produced by the hydrothermal-assisted method were denoted as LZ-HTA, and in comparison, the particles produced only via high temperature calcination were marked as LZ-UHTA.

2.2. Hot corrosion resistance tests

Hot corrosion resistance tests on the LZ-HTA and LZ-UHTA particles were performed simultaneously. The V_2O_5 was used as the hot corrosion agent. The mixture consisting of V_2O_5 (10 wt%) and LZ particles (90 wt%) was heated at 1473 K in an air electric furnace. Following a 2-h dwell time, the specimens were furnace-cooled down to room temperature.

2.3. Characterization of LZ

The phase structure of the as-synthesized LZ was identified by the Fourier transform infrared spectra (FT-IR, model:

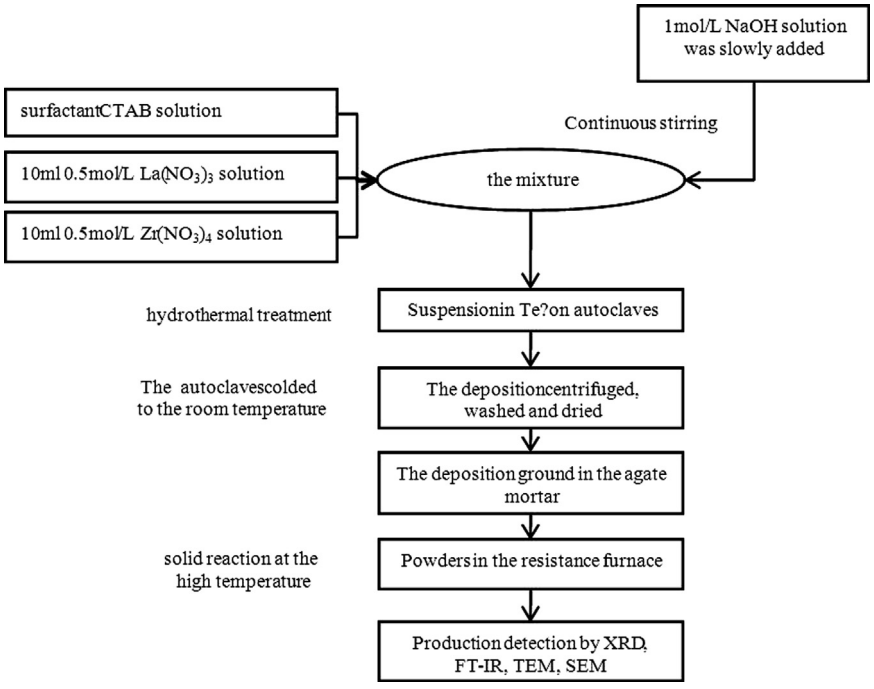

Fig. 1. The fabrication process of the nano LZ particles.

Spectrum) with KBr as solid solvent and particle X-ray diffraction (XRD, model: D-8X Advance) instrument with a Cu Ka target giving a monochromatic beam, and the wavelength and the scanning rate were 1.5406 Å and 2° min^{-1}, respectively. The XRD operation voltage and current were maintained at 40 kV and 40 mA, respectively. The lattice parameters were determined by a least-squares refinement. The particles morphology was evaluated by Transmission Electron Microscopy (TEM, model: HITACHI, H-7650) and the particles morphology after V_2O_5 hot corrosion was obtained by Scanning Electron Microscopy (SEM, model: HITACHI S-4300). The thermal behavior of the dried particles was studied from 373 to 1473 K in the nitrogen environment using thermo gravimetric and differential thermal analysis (TG/DTA, model: Perkin-Elmer Diamond) with a heating rate of 10 K min^{-1}. The distribution of particle clusters of finely ground slag was measured by means of a laser granulometer (model: Zetasizer Nano ZS90).

3. Results and discussion

3.1. The characterization of the process of LZ synthesis

The TG/DTA analysis of the dry powders coprecipitated from the mixture solution of $Zr(NO_3)_4$ and $La(NO_3)_3$ is shown in Fig. 2. The DTA curve shows a sharp endothermic peak around 381 K, which involves a mass loss of 3% of the mixture. Such a peak is attributed to the evaporation of occluded water in the sediment. Meanwhile, an endothermic peak centered about 652 K can be observed in the curve, corresponding to the elimination of the bound water in the composition containing the Zr^{4+} and La^{3+} with a mass loss of 7–9%. At the point corresponding to 761 K in the DTA curve, there is endothermic peak from the decomposition of the zirconium hydroxide and crystallization of the cubic zirconia. And at the point corresponding to the 905 K in the curve, another endothermic peak exists due to the decomposition from lanthanum hydroxide to the lanthana and water eliminated from the solid particles. Above the 905 K, no obvious weight loss can be observed in the TG curve. Moreover,

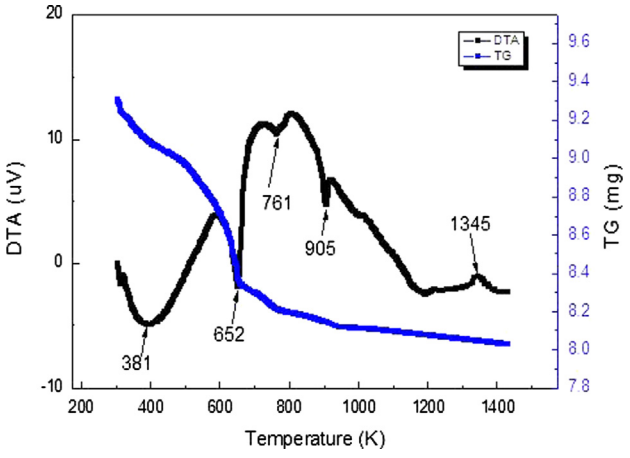

Fig. 2. TG/DTA diagram of the precipitate mixtures.

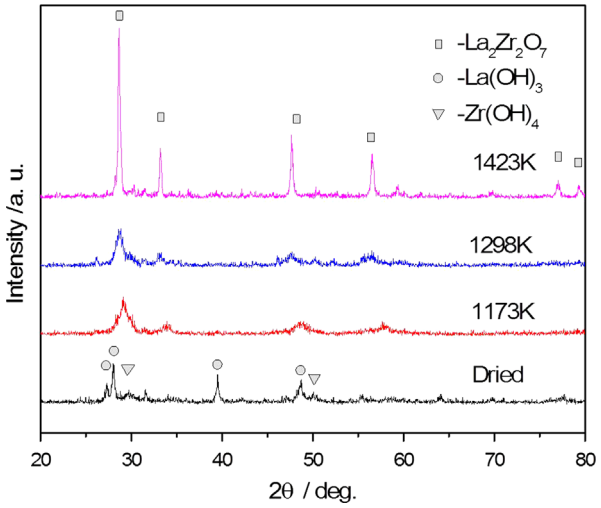

Fig. 3. XRD patterns of the products with different solid reaction temperatures.

a small exothermal peak appears above 1183 K in the DTA curve and the peak value exists at 1345 K, at which temperature a solid phase reaction of zirconia and lanthana occurs to form lanthanum zirconate (LZ).

In this work, nano LZ crystals were obtained by calcining the hydrothermal particles at different temperatures, 1173 K, 1298 K and 1423 K, according to the TG/DTA results in Fig. 2. The three temperatures, which are higher than three key points (905 K, 1183 K and 1345 K) in Fig. 2, were selected in order to investigate the influence of temperatures on the solid-reaction process of nano LZ particles. The XRD patterns of the products are shown in Fig. 3. It can be seen that the dried precipitate mixtures at room temperature are composed of $La(OH)_3$ and $Zr(OH)_4$ which come from reaction between OH^- in the NaOH solution and cations in the precursors solution. As the temperature was increased to 1173 K, the peaks corresponding to $La(OH)_3$ and $Zr(OH)_4$ disappeared, and a single LZ phase was formed and no extra peak was observed, which indicated that pure LZ with pyrochlore structure could be synthesized at lower temperature via the hydrothermal assisted method compared to the conventional solid reaction process.

The mean size of the particles was determined by Scherrer's equation

$$D = \lambda \frac{K}{\beta \cos \theta} \quad (1)$$

where D is the mean diameter of the particles, λ is the wavelength of X-ray radiation (0.154056 nm), θ is the diffraction angle, K is a constant (0.89), and β is the corrected full-width half maximum (FWHM) [9,16]. The mean diameters of the particles solid-reacted at 1423 K, 1298 K, and 1173 K are 11.67 nm, 3.09 nm and 2.02 nm, respectively. It is indicated that the size of the LZ particles increased with the increase of the solid reaction temperatures, but every size is less than 100 nm. Moreover, with the increase of the solid-reaction temperature from 1173 K to 1423 K, the peak intensity of the LZ in XRD patterns becomes stronger, which implies the well growth of crystal at higher temperature. When the temperature

was increased up to 1423 K, the peaks (77° and 79°) corresponding to LZ (JCPDS: 73-0444) with pyrochlore structure appeared, indicating that 1423 K is an appropriate solid reaction temperature to produce the nano LZ particles with pyrochlore structure.

Based on the results of TG/DTA, XRD analysis, the reaction equation can be expressed as follows:

$$Zr(OH)_4 \rightarrow ZrO_2 + 2H_2O\uparrow \ 761\ K \quad (2)(2)$$

$$2La(OH)_3 \rightarrow La_2O_3 + 3H_2O\uparrow \ 905\ K \quad (3)(3)$$

$$2ZrO_2 + La_2O_3 \rightarrow La_2Zr_2O_7 \ 1345\ K \quad (4)(4)$$

It is well known that the particles can grow rapidly to form the sintered hard agglomerate at higher temperature. Therefore, the solid reaction temperature should be as low as possible in order to produce the nanosize LZ particles. Based on the XRD patterns, the pyrochlore structure can be formed at 1423 K, and the mean size of the as-calcined particles is about 12 nm. As a consequence, the best temperature to calcine the as-hydrothermal particles was selected as 1423 K.

3.2. Mechanism of the hydrothermal treatment

Different temperatures in the hydrothermal experiments were used to investigate the effect of hydrothermal temperatures on the construction and component of nano LZ particles. All the as-hydrothermal products were calcined at 1423 K for 2 h in electrical resistance furnace and then were tested by FT-IR and XRD. The FT-IR spectra and XRD patterns of products at different hydrothermal temperatures are shown in Fig. 4. The FT-IR spectrum curves of the as-prepared LZ hydrothermally treated at different temperatures are shown in Fig. 4a. Several characteristic absorption bands can be observed at about 506, 1385, 1490, 1632 and 3609 cm^{-1}. The detection of absorption bands centered at about 3609 cm^{-1} is an evidence of residual water molecules contained in the particles, and the absorption band at 1632 cm^{-1} represents another vibration of water molecules. The band at 506 cm^{-1} is attributed to Zr–O bonds existed in LZ or ZrO_2. These bands are similar in FT-IR

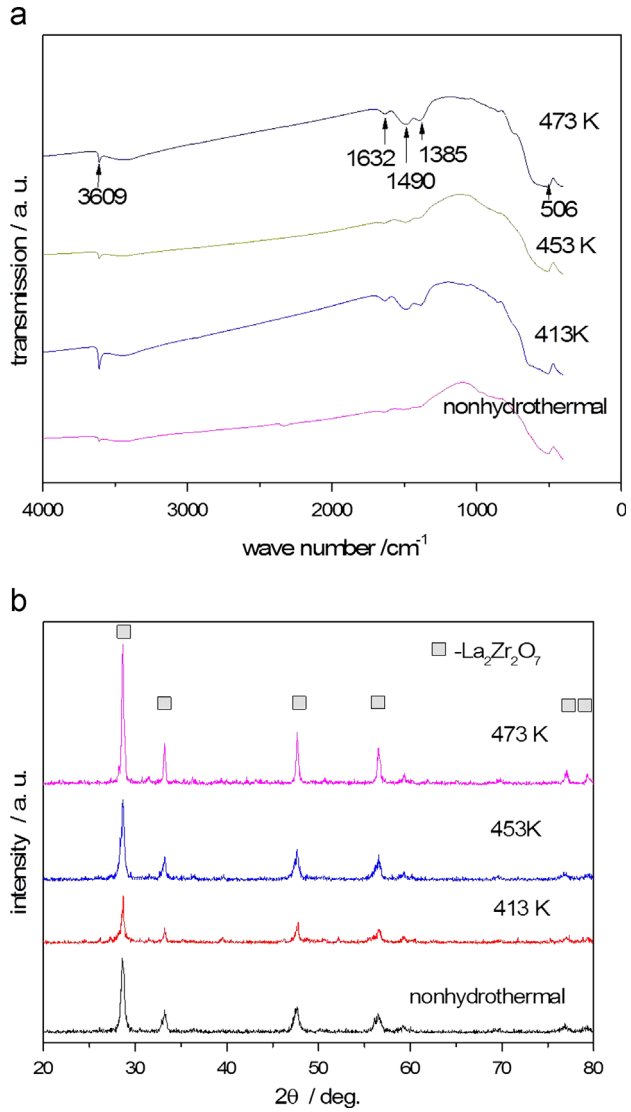

Fig. 4. FT-IR spectra (a) and XRD patterns (b) of LZ with different hydrothermal temperatures.

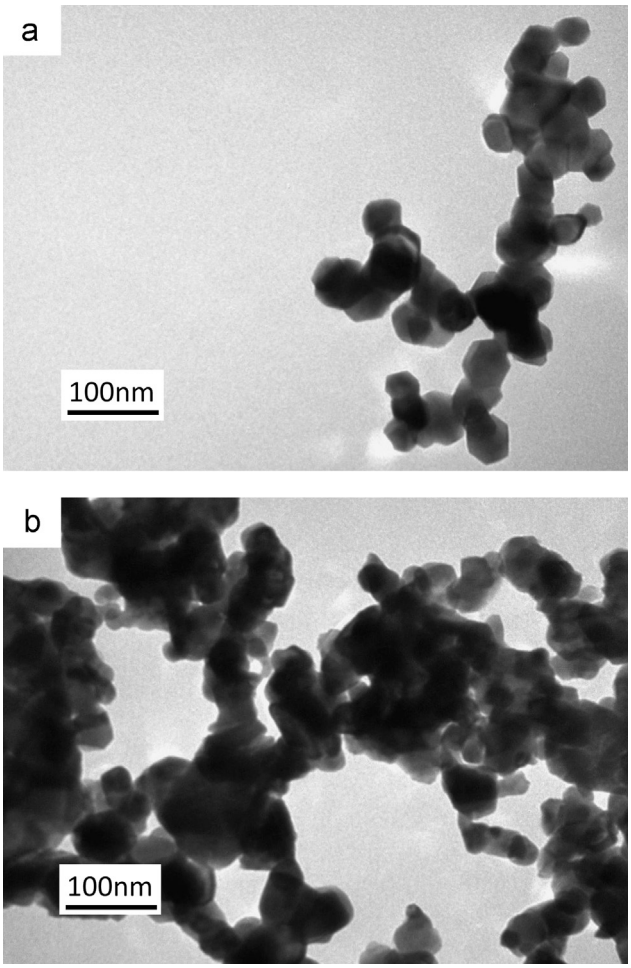

Fig. 5. TEM image of as-calcined particles: (a) LZ-HTA (hydrothermal temperature 453 K for 24 h and sintered at 1423 K) and (b) LZ-UHTA.

spectra with different hydrothermal treatments, and it can be seen that the formation of the Zr–O bonds is independent of the hydrothermal temperature. In the spectra, the band located at 1076–1101 cm^{-1} assigned to the formation of nitrate complexes do not exist, which indicated that the nitrate in the Zr^{4+} and La^{3+} precursors has decomposed. The band at 1490 cm^{-1} resulted from La–O vibration appeared in the spectra of the specimen via the hydrothermal treatment. It is reasonable to draw a conclusion that the hydrothermal treatment can affect the La–O bond formation. The intensities of diffraction peaks increase gradually with increasing the hydrothermal temperatures from 413 K to 473 K, seen in Fig. 4b, which indicates that the crystallinity of LZ particles increases with increasing the hydrothermal temperature. The hydrothermal temperature can affect the crystal nucleation and growth in the high pressure environment [9]. The higher temperature is helpful to crystal growth because higher temperature can provide more energy and higher pressure which can accelerate the reaction between the two kinds of compounds containing the cations of Zr and La respectively.

The TEM images of the as-prepared LZ particles are shown in Fig. 5. The LZ-HTA (Fig. 5a) was prepared by two steps consisting of hydrothermal treatment at 453 K for 24 h and high temperature calcination at 1423 K for 2 h. In comparison, LZ-UHTA (Fig. 5b) was prepared only by high temperature calcination at 1423 K for 2 h. The LZ-HTA particle is regular hexahedron in the shape in accord with unit cell of LZ, and particle size (10–30 nm) of LZ-HTA with the hydrothermal treatment is relatively smaller than that of the size (30–50 nm) of LZ-UHTA. It also indicated that the nanoparticles via the hydrothermal treatment are better dispersed in alcohol by supersonic. Some soft agglomerates, produced by uncontrolled agglomeration in the process of precipation[9], can be observed in the nano LZ particles (Fig. 5). In Fig. 6, the results show that the mean agglomerate size (277.9 nm, seen in Fig. 6a) of LZ-HTA is smaller than that of LZ-UHTA (1061 nm, seen in Fig. 6b). It can be further concluded that the hydrothermal treatment can be beneficial to grow nano-compound particles and to improve the dispersity of nanoparticle.

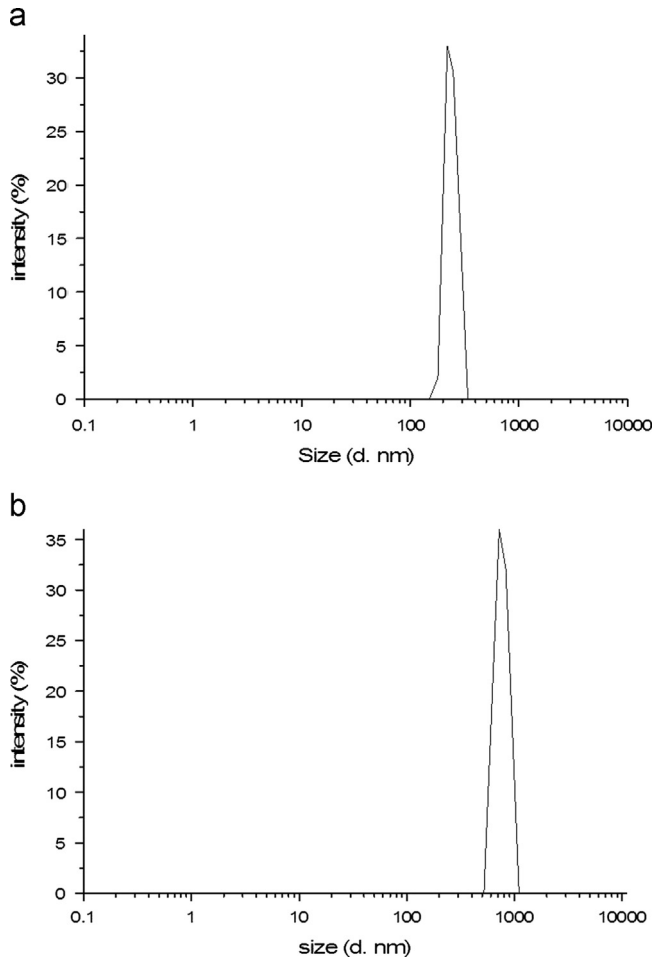

Fig. 6. Agglomerates size distributed patterns of the nano LZ particles in alcohol by ultrasonic vibration for 2 h. (a) LZ-HTA at 453 K for 24 h and sintered at 1423 K whose mean agglomerate size is 277.9 nm and (b) LZ-UHTA whose mean agglomerates size is 1061 nm.

The schematic diagram of the nano LZ processing in the hydrothermal treatment and solid reaction is shown in Fig. 7. According to the above XRD, TEM, and FT-IR analyses, the processing can be described as follows: (1) the two kinds of particles obtaining Zr and La can blend well with enhanced convection of the water in the hydrothermal vessel as the hydrothermal temperature rises (Fig. 7a); (2) the uniform aggregation made of the two kinds of particles is performed by electrostatic force of the cationic surfactant (Fig. 7b); (3) the aggregations were compacted under the high pressure at hydrothermal condition, which can be beneficial to accelerate the solid reaction due to the increasing of the interface area between the two kinds of deposition (Fig. 7c); and (4) the surfactant can avoid the reaction among the small aggregations to obtain the nanosize particles although it can be burnt off (Fig. 7d and e).

3.3. Hot corrosion resistance analysis

In order to investigate high temperature corrosion resistance of LZ particles, the mixture of 10 wt% V_2O_5 and 90 wt% nano LZ particles were calcined at 1473 K for 2 h. Two kinds of nano LZ particles, LZ-HTA and LZ-UHTA, are used separately. LZ-HTA particles were prepared by two steps consisting of hydrothermal treatment at 453 K for 24 h and calcination at 1423 K for 2 h. LZ-UHTA particles were only calcined at 1423 K for 2 h.

The XRD patterns of the V_2O_5 hot corrosion products of the LZ particles and the as-prepared LZ particles are shown in Fig. 8. The XRD patterns of LZ-HTA particles have less change after V_2O_5 hot corrosion (Fig. 8c), and the corrected FWHM decreased from 0.351° to 0.289° which indicates that the particles size increased slightly from 23.1 to 28.1 nm after V_2O_5 hot corrosion according to Eq. (1). The XRD patterns of LZ-UHTA particles showed obvious change after V_2O_5 hot corrosion. The value of the main diffraction peak declined significantly, and the corrected FWHM decreased from 0.332° to 0.212°. The grain size of LZ-UHTA particles increases from 24.4 nm to 38.6 nm. It can be concluded that the V_2O_5 hot

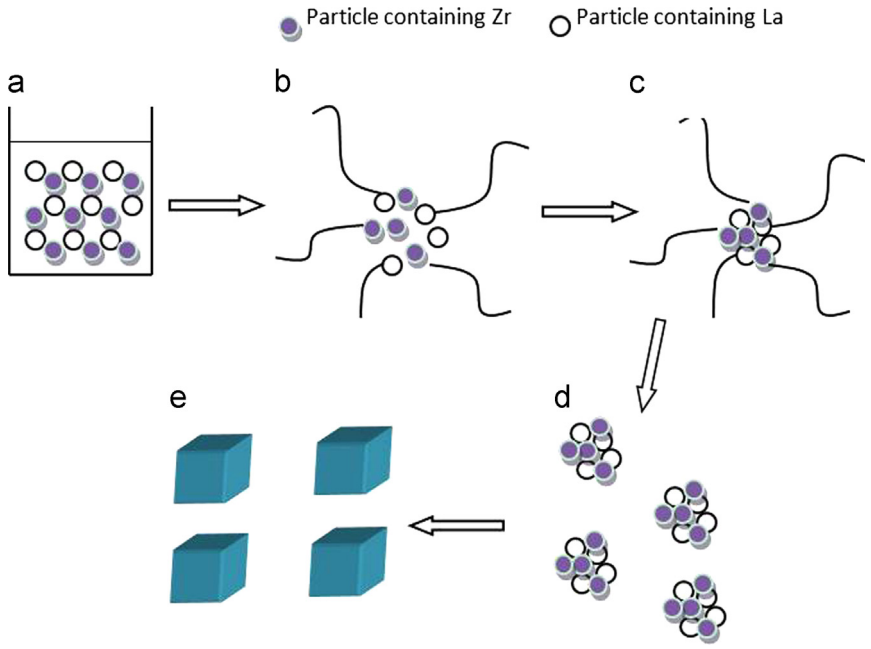

Fig. 7. The schematic diagram of the nano LZ processing in hydrothermal treatment and solid reaction. (a) well dispersion, (b) aggregation, (c) Densification under hydrothermal condition, (d) High temperature solid reaction and (e) Regular nano $La_2Zr_2O_7$ crystal.

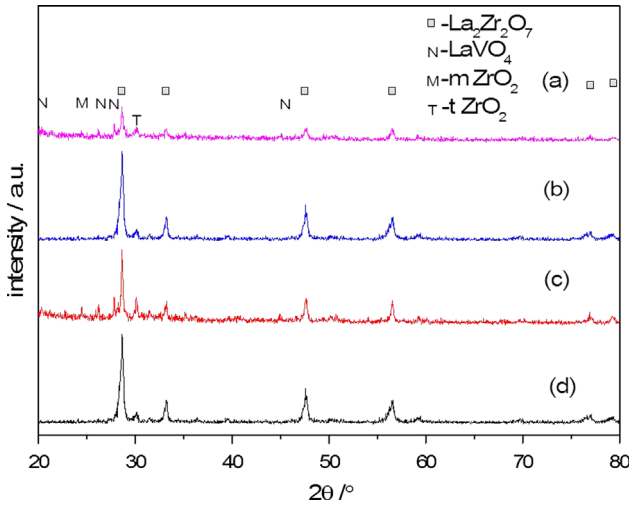

Fig. 8. XRD patterns comparison of LZ via V_2O_5 hot corrosion. (a) LZ-UHTA particles by V_2O_5 hot corrosion; (b) initial LZ-UHTA particles; (c) LZ-HTA particles by V_2O_5 hot corrosion; and (d) initial LZ-HTA particles.

corrosion can accelerate the grain growth rate of the LZ particles without the hydrothermal treatment. It is found that LZ reacts with molten V_2O_5 to form $LaVO_4$ as the major corrosion product in Fig. 8a and c. The formation of the corrosive products resulted from the disruptive LZ phase transformation partially from pyrochlore to tetragonal and monoclinic phase ZrO_2 (M ZrO_2). A possible reaction that could have produced these phases can be written as [17]

$$La_2Zr_2O_7(s)+V_2O_5(l)\rightarrow 2LaVO_4(s)+2ZrO_2(s) \quad (5)(5)$$

The SEM photographs of two kinds of LZ particles via V_2O_5 hot corrosion are shown in Fig. 9. The grain size of the as-prepared nano LZ-UHTA particles (Fig. 9b) is about 45 nm, crystalline shape is irregular, and agglomeration is obvious. However the grain size of the as-prepared nano LZ-HTA particles (Fig. 9d) is about 30 nm which is smaller than that of LZ-UHTA particles. The crystalline shape is regular, and the dispersion is well. Via V_2O_5 hot corrosion at 1473 K for 2 h, the LZ-UHTA particles had a remarkable agglomeration and the surface turn into interface, but the LZ-HTA particles grew uniformly and had less agglomeration (Fig. 9c). The results show that the nano LZ-HTA particles have better corrosion resistance than the nano LZ-UHTA. The reason for corrosion resistance of nano LZ-HTA particles could be that crystalline of LZ-HTA particles grew perfectly and compactly to form less detect structure by hydrothermal treatment, then the structure can effectively prevent the LZ particles from the V_2O_5 corrosive invasion. In actual application on the TBCs, the better hot corrosion V_2O_5 resistance property of the nano LZ is necessary to elevate the V_2O_5 and hot resistance of the TBCs [18]. Therefore, the LZ-HTA particles are more suitable to produce the nanostructured TBCs.

4. Conclusions

The nano LZ particles with pyrochlore structure were successfully prepared in the current study. The effect of the hydrothermal-assisted method on the crystal size, shape and V_2O_5 hot corrosion resistance of LZ particles were evaluated. Some important results can be summarized as follows:

(1) It was found that the hydrothermal temperature and the solid reaction temperature have an important influence on the formation of nanocrystal of the product. The crystallinity of

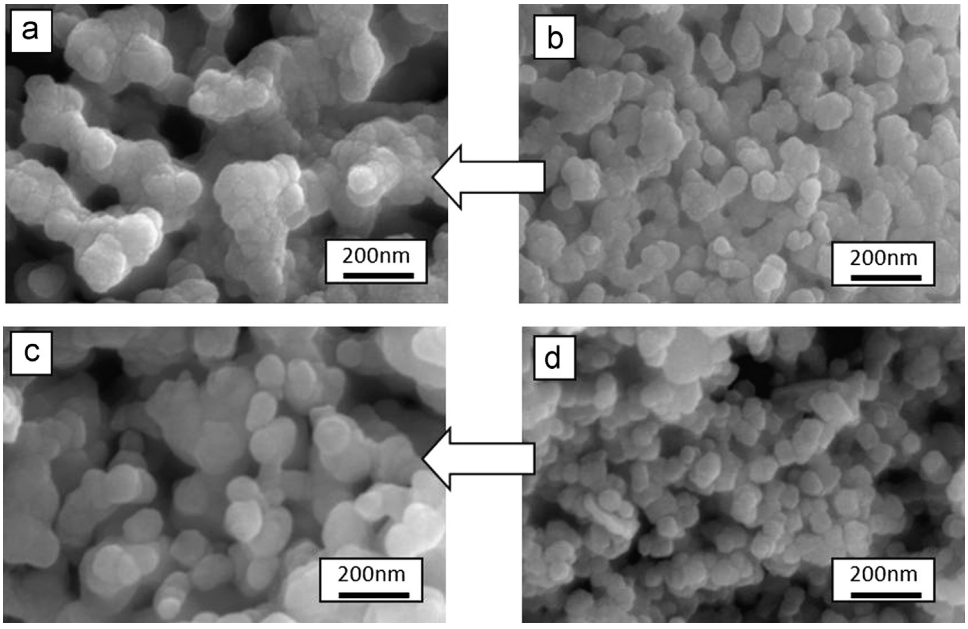

Fig. 9. SEM photograph comparison of LZ before and after V_2O_5 hot corrosion. (a) LZ-UHTA particles by V_2O_5 hot corrosion; (b) as-prepared LZ-UHTA particles; (c) LZ-HTA particles by V_2O_5 hot corrosion; and (d) as-prepared LZ-HTA particles.

LZ particles increases with increasing hydrothermal temperature. With the increase of the solid-reaction temperature from 1173 K to 1423 K, the peak intensity of the LZ in XRD patterns becomes stronger, which implies the well growth of crystal at higher temperature. 1423 K is an appropriate solid reaction temperature to produce the nano LZ particles with pyrochlore structure.

(2) The LZ particles with the hydrothermal treatment have better hot corrosion resistance properties and it is suitable to produce the nanostructured LZ TBCs. LZ reacts with molten V_2O_5 to form $LaVO_4$ as the major corrosion product. Crystalline of LZ-HTA particles grew perfectly and compactly to form less detect structure by the hydrothermal treatment, then the structure can effectively prevent the LZ particles from the V_2O_5 corrosive invasion.

Acknowledgments

This work is supported by the Young Scientist Project of Natural Science Foundation of China (NSFC) under Grant no. 51202277 and the program for Young Teachers Scientific Research in Qiqihar University (2011k-M24).

References

[1] M. Uno, A. Kosuga, M. Okui, K. Horisaka, H. Muta, K. Kurosaki, S. Yamanaka, Photoelectrochemical study of lanthanide zirconium oxides, $Ln_2Zr_2O_7$ (Ln=La, Ce, Nd and Sm), Journal of Alloys and Compounds 420 (2006) 291–297.

[2] H.C. Gupta, S. Brown, An analytical expression for Eg and Ag modes of pyrochlores, Journal of Physics and Chemistry of Solids 64 (2003) 2205–2207.

[3] L. Wang, Y. Wang, X.G. Sun, J.Q. He, Z.Y. Pan, L.L. Yu, Preparation and characterization of nanostructured $La_2Zr_2O_7$ feedstock used for plasma spraying, Powder Technology 212 (2011) 267–277.

[4] H.Y. Jin, D. Huang, Q. Gao, L. Li, N. Wang, Y.Q. Wang, S.E. Hou, Synthesis of lanthanum zirconium oxide nanomaterials through composite-hydroxide-mediated approach, Materials Research Bulletin 47 (2012) 51–53.

[5] Y.P. Tong, J.W. Zhu, L.D. Lu, X. Wang, X.J. Yang, Preparation and characterization of $Ln_2Zr_2O_7$ (Ln=La and Nd) nanocrystals and their photocatalytic properties, Journal of Alloys and Compounds 465 (2008) 280–284.

[6] A.Y. Zhang, M.K. Lu, G.J. Zhou, S.M. Wang, Y.Y. Zhou, Combustion synthesis and photoluminescence of Eu^{3+} and Dy^{3+}-doped $La_2Zr_2O_7$ nanocrystals, Journal of Physics and Chemistry of Solids 67 (2006) 2430–2434.

[7] X.R. Cheng, Z.M. Qi, T.T. Li, G.B. Zhang, C.X. Li, H.J. Zhou, Y.Y. Wang, M. Yin, Infrared phonon modes and dielectric properties of $La_2Zr_2O_7$: comparing thin film to bulk material, Physica Status Solidi B 249 (2012) 854–857.

[8] Z.H. Xu, S.M. He, L.M. He, R.D. Mu, G.H. Huang, X.Q. Cao, Novel thermal barrier coatings based on $La_2(Zr_{0.7}Ce_{0.3})_2O_7$/8YSZ double-ceramic-layer systems deposited by electron beam physical vapor deposition, Journal of Alloys and Compounds 509 (2011) 4273–4283.

[9] C.J. Wang, Y. Wang, Y.L. Cheng, L. Zhu, B.L. Zou, Y. Zhao, W.Z. Huang, X.Z. Fan, Z.S. Khan, X.Q. Cao, Synthesis of nanocrystalline La_2O_3–Y_2O_3–ZrO_2 solid solutions by hydrothermal method: a crystal growth and structural study, Journal of Crystal Growth 335 (2011) 165–171.

[10] M.O.D. Jarligo, Y.S. Kang, A. Kawasaki, Physicochemical properties of single phase $La_2Zr_2O_7$ particle, Materials Transactions 46 (2005) 189–192.

[11] K.K. Rao, T. Banu, M. Vithal, G.Y.S.K. Swamy, K.R. Kumar, Preparation and characterization of bulk and nanoparticles of $La_2Zr_2O_7$ and $Nd_2Zr_2O_7$ by sol–gel method, Materials Letters 54 (2002) 205–210.

[12] Y.P. Tong, L. Lu, X.J. Yang, X. Wang, Characterization and their photocatalytic properties of $Ln_2Zr_2O_7$ (Ln=La, Nd, Sm, Dy, and Er) nanocrystals by the stearic acid method, Solid State Sciences 10 (2008) 1379–1383.

[13] Y.P. Tong, Y.P. Wang, Salt-assisted combustion synthesis of nanocrystalline $Nd_2(Zr_{1-x}Sn_x)_2O_7$ ($0 \le x \le 1$) solid solutions, Materials Characterization 60 (2009) 1382–1386.

[14] X. Wu, J. Chen, Z. Shi, H. Huang, L. Liu, J. Yu, Y. Zou, G. Li Y. Zhao, Hydrothermal synthesis and photoluminescence properties of $BaZr_{1-x}Ti_xO_3$ hollow nanospheres, Materials Letters 86 (2012) 21–24.

[15] K. Byrappa, T. Adschiri, Hydrothermal technology for nanotechnology, Progress in Crystal Growth and Characterization of Materials 53 (2007) 117–166.

[16] P. Zhang, A. Navrotsky, B. Guo, I. Kennedy, A.N. Clark, C. Lesher, Q.Y. Liu, Energetics of cubic and monoclinic yttrium oxide polymorphs: phase transitions, surface enthalpies, and stability at the nanoscale, Journal of Physical Chemistry C 112 (2008) 932–938.

[17] S. Yugeswaran, A. Kobayashi, P.V. Ananthapadmanabhan, Hot corrosion behaviors of gas tunnel type plasma sprayed $La_2Zr_2O_7$ thermal barrier coatings, Journal of the European Ceramic Society 32 (2012) 823–834.

[18] L. Wang, Y. Wang, X.G. Sun, J.Q. He, Z.Y. Pan, C.H. Wang, Finite element simulation of residual stress of double-ceramic-layer $La_2Zr_2O_7$/8YSZ thermal barrier coatings using birth and death element technique, Computational Materials Science 53 (2012) 117–127.